About this Article

This material was included with the downloadable supplemental content accompanying the *ARRL Antenna Book*.

You may print a copy of this material for personal use. Any other use of the information requires permission from the ARRL.

Copyright/Reprint Notice

Kai Siwiak, KE4PT and **Richard Quick, W4RQ**
10988 NW 14th St., Coral Springs, FL 33071; **k.siwiak@ieee.org** 695 Fairway Dr., Plantation, FL 33317; **w4rq@arrl.net**

Small Gap-resonated HF Loop Antenna Fed by a Secondary Loop

Improved formulas for the loop current and loop impedance lead to an accurate determination of close-near-fields, and far field null depths.

The small gap-resonated high frequency circular loop antenna has received much attention in Amateur Radio since John H. Dunlavy, Jr. patented[1] his efficient small loop that can be tuned over wide bandwidths. The now-expired patent spawned a multitude of homebrew loops and several commercial products aimed at hams.

Loop analysis dates back to the earliest days of radio with Pocklington's 1897 paper[2] on the thin wire loop. Later Hallén[3] expanded on the receiving qualities of loops, and Storer[4] studied the impedance of thin wire loops. Loop analysis was generalized[5] by Q. Balzano and one of us, Kai Siwiak, KE4PT, to fat wires giving, among other results, the details of current density along the circumference as well as the cross-section of the loop wire. The results here are derived from the Balzano-Siwiak work, and specialized[6] to electrically small loops. We relied on the Neumann formula[7] to find the mutual coupling between the primary and the secondary feeding loops. We also report on the effects of common mode currents (CMCs) coupling to the feeding coax cable, as well as mutual coupling of the loop to the ground. We verified our analytical results by simulations using Numerical Electromagnetic Code (NEC) models in 4*nec*2 software[8]. Our NEC model includes the primary loop, the secondary feeding loop, a resonating capacitor, and a conductor representing the shield of the coaxial feed line.

We present results rather than lengthy derivations that can be gleaned from the referenced notes. In Section (1) we show the loop current density along the loop circumference and in the cross section, revealing current bunching. In Section (2) we present the loop impedance, including effects of loop wire thickness, and non-uniform loop current. In Section (3) we show the effect of the secondary feeding loop. In Section (4) we provide details about the loop near fields and far-field null filling that are a direct result of considering the non-uniform loop current. In Section (5) we show the effects of loop currents coupling to a coaxial feed line shield. In Section (6) we calculate coupling of the loop to the ground. In Section (7) we determine the loop efficiency. We conclude with a summary in Section (8).

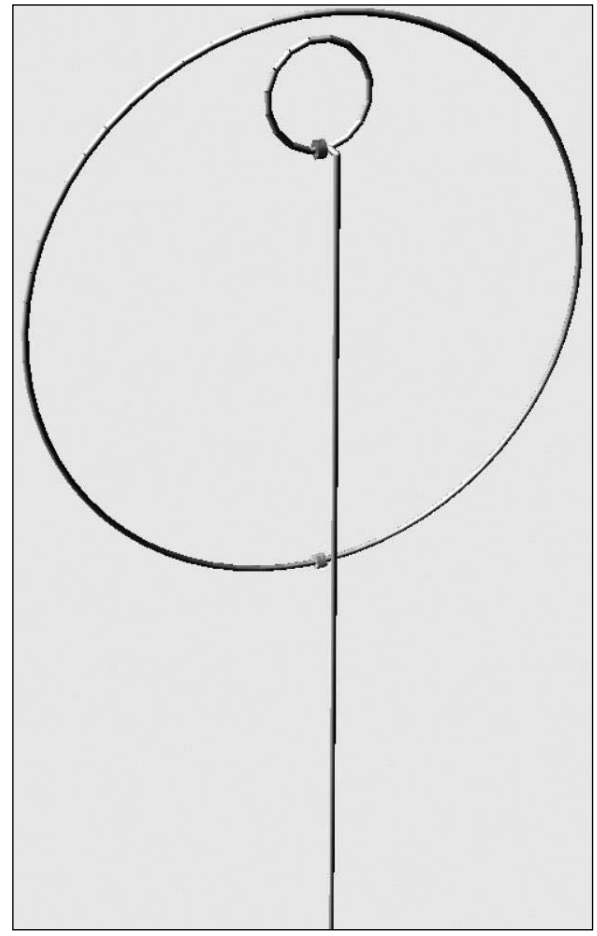

Figure 1 — The electrically small HF loop includes a primary loop and a secondary feeding loop, both in the same *zx*-plane, and a coaxial cable feed line also in the *zx*-plane, but slightly displaced in the *y*-axis, so that the cable does not touch the bottom of the primary loop. A resonating capacitor connects across a gap at the bottom of the primary loop.

1 — Small Loop Currents and Fields

The circular loop geometry for our study is shown in Figure 1, rendered in 4*nec*2 software. The primary loop diameter is 2*b*, the loop

wire diameter is $2a$, the angular extent along the loop circumferences is ϕ, with the loop gap located at $\phi = 0°$. The resonating capacitor is connected across the gap at the bottom of the primary loop. The secondary feeding loop is $2b_2$ in diameter and with $2a_2$ conductor diameter. A coaxial cable feed connects across a gap at the bottom of the smaller secondary loop. We studied the effect of currents coupling to the coax cable shield by varying the length of that coax.

The variation around the loop wire cross-sectional circumference is angle ψ with $\psi = 0°$ pointing to the outside of the loop. We examine a specific loop with $a = 0.00406$ m, $b = 0.4534$ m (loop circumference is 2.85 m), $a_2 = 0.002$ m, and $b_2 = 0.077$ m. The loop centers were displace by 0.343 m. We varied the length of the coax feed line for the common mode current coupling portion of the study. Our loop dimensions closely match those of the *AlexLoop*[9] by Alex Grimberg, PY1AHD.

1.1 — The Dunlavy Loop

John Dunlavy discovered that a loop antenna comprising a one turn primary loop having a circumference of less than three-eighths of a wavelength and interrupted along its length by a gap, with a tuning capacitor connected across the gap, can be tuned by up to a 10:1 tuning range. A single-turn secondary loop, much smaller than the primary loop, is inductively coupled to the primary loop. Both loops are in the same plane. The secondary loop diameter is selected to bear an optimum relationship to the diameter of the primary loop so that variation in feed impedance is minimized over the band of operation. A low impedance transmission line (50 Ω) connects to the terminals of the secondary loop.

Dunlavy used relatively thick conductors of copper or aluminum, and a construction that minimized excessive resistive losses.

1.2 — Loop Current Density

The loop current density $J(\phi, \psi)$ is a Fourier series in terms of $\cos(n\phi)$ along the loop circumference and $\cos(m\psi)$ along the cross-sectional circumference. We initially retained just the $m = n = 0$ and 1 terms. The $m = 1$ term reveals current bunching on the inner surface of the loop conductor. The $n = 1$ term accounts for the first order variation of the circumferential loop current. Including that term reveals details about the close-near fields, and about the far-field peak-to-null ratio. The current density is,

$$J(\phi,\psi) = \frac{I_0}{2\pi a}\left\{1 - 2(kb)^2\cos(\phi)\right\}\left\{1 + Y(a,b)\cos(\psi)\right\} \quad (1)$$

The first curly brackets contain the circumferential variation of the current in ϕ. The second curly brackets include the function $Y(a, b)\cos(\psi)$, which describes current bunching in the cross-sectional circumference of the loop conductor. These curly-bracket terms are ignored in most previous formulas for loop current density. From Note 6 a curve-fit approximation for Y is,

$$Y(a,b) = -\left(\frac{2a}{10a+b}\right)^{0.75} \quad (2)$$

which when multiplied by $\cos(\psi)$ integrates to zero in the ψ-directed cross sectional circumference of the loop conductor. In our example values of a and b, $Y = -0.046$, indicating less than 5% current bunching on the inner surface of the loop conductor. Since our loops have an a to b ratio of less than 0.009, we will not consider the current bunching in the ψ direction any further.

Integrating the current density over the loop conductor cross section in ψ, and noticing that the circumference in wavelengths $kb = 2\pi b/\lambda = C_\lambda$, we see that the loop current is,

$$I(\phi) = I_0\left\{1 - 2C_\lambda{}^2\cos(\phi)\right\} \quad (3)$$

which instantly reveals that the first order current amplitude variation term depends solely on the loop circumference in wavelengths. The loop current Eqn. (3) is valid for $C_\lambda < 0.3$, and is used to solve for the loop fields in classic fashion.

Figure 2 shows the loop current for the 2.85 m circumference loop at 7, 14, and 30 MHz, where C_λ is 0.067, 0.133, and 0.285 respectively. The variation increases with frequency.

1.3— General Form of the Loop Fields

With reference to the details in Note 5, the electric and magnetic fields are obtained from the vector **A** and scalar V potentials in classical fashion,

$$\mathbf{E} = -\nabla V - j\omega\mathbf{A} \quad (4)$$

$$\mathbf{H} = \frac{1}{\mu_0}\nabla\times\mathbf{A} \quad (5)$$

The boundary conditions require that tangential electric fields are zero on the loop surface everywhere except at the loop gap. The components of the vector potential in cylindrical coordinates are,

$$A_\phi = \frac{1}{4\pi}\iint_{S'} J_\phi\cos(\phi-\phi')GdS' \quad (6)$$

$$A_\rho = \frac{1}{4\pi}\iint_{S'} J_\phi\sin(\phi-\phi')GdS' \quad (7)$$

and the scalar potential is,

$$V = \frac{j\eta_0}{4\pi\varepsilon_0 k}\iint_{S'}\frac{1}{\rho'}\frac{\partial J_\phi}{\partial\phi'}GdS' \quad (8)$$

The integrals are over the surface S' of the loop wire. The intrinsic impedance of free space is $\eta_0\,\Omega$, and $k = 2\pi/\lambda$ m^{-1} is the wave number, and ε_0 F/m is the free space permittivity. The Green's function is,

$$G = \frac{e^{-jk|\mathbf{r}-\mathbf{r}'|}}{|\mathbf{r}-\mathbf{r}'|} \quad (9)$$

where $|\mathbf{r}-\mathbf{r}'|$ is the distance between the field point and the current density point on the wire. We solved these equations in a *Mathcad* spread sheet, and the details are available on the **www.arrl.org/qexfiles** web page. The results are valid from the surface of the loop conductor to everywhere in space. We also validated these analytical results with simulations using an NEC model rendered in 4*nec*2 software, see Table 1, also on the **/qexfiles** web page. The NEC model includes the primary loop, the secondary feeding loop, a length of wire representing the shield of the coax cable feed line, and a resonating capacitor.

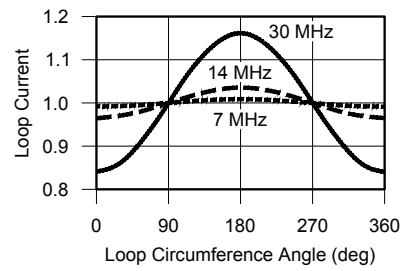

Figure 2 — Loop currents at 7, 14, and 30 MHz along the loop circumference vary in amplitude due to the inclusion of a Fourier series expansion term.

Table 1.

Numerical Electromagnetic Code (4nec2) model includes the primary loop, a secondary feeding loop and segment of wire representing the shield of the coax cable feed line, and a resonating capacitor.

```
CM                                      Frequency - frq MHz
CM                                      Includes feed stub; (1+j0)V source
CM                                      RG-213/U primary loop, Rloss aluminum
CM                                      RG-58/U coupling loop
CM                                      No Ground
CE
SY frq=14.10                            'frequency MHz
SY b=0.45339                            'primary loop radius, m
SY a=0.004064                           'Primary loop wire radius, m
SY b2=0.077                             'Feed loop radius, m
SY a2=0.002                             'Feed loop wire radius, m
CM
SY C=43.40e-12                          'INPUT RESONATING CAPACITOR, Farad
CM
SY Qc=2400                              'Input resonating capacitor Q
SY Rp=Qc/(2*3.1415926535*frq*1e6*C)     'Parallel equivalent capacitor resistance
SY cond=34000000                        'aluminum, RC-213/U shield conductivity
SY n=64                                  'Input n-polygon primary loop
SY n2=16                                'Input n-polygon coupling loop
SY ang1b=-90-360/(2*n)                  'start of arc angle of primary loop
SY ang2b=ang1b+360                      'end of arc of primary loop
SY ang1b2=-90-360/(2*n2)                'start of arc angle of feed loop
SY ang2b2=ang1b2+360                    'end of arc angle of feed loop
SY zb=1.5                               'elevation in Z of center of loop
SY loopgap=4.5*(a+a2)                   'gap between primary and feed loop
SY zb2=zb+0.343038                      'elevation in Z of center of feed loop
CM
SY nstub=1                              'CHOOSE number of stub segments
CM                                      nstub=34 for 1.5 m cable; 74 for AlexLoop 129 inch coax length
SY stublength=0.0445*nstub              'compute stub 'SEGMENT LENGTH FIXED AT 0.0445 m
SY stubZ=1.7675                         'stub start coordinate
SY sEnd=stubZ-stublength                'stub end coordinate
CM                                      primary loop arc, GA, shifted in Z
GA  1  n      b              ang1b   ang2b   a
GM  0  0      0              0       0       0              0     zb     1
GA  2  n2     b2             ang1b2  ang2b2  a2
GM  0  0      0              0       0       0              0     zb2    2
CM
GW  3  1      -0.0150219548  0       stubZ   -0.0150219548  0.03  stubZ  a2
GW  4  nstub  -0.0150219548  0.03    stubZ   -0.0150219548  0.03  sEnd   a2
GE  0
LD  1  1      1              1       Rp      0              C
LD  5  0      0              0       cond
GN  -1
EK
EX  0  2      1              0       1.      0.0
FR  0  0      0              0       frq     0
EN
```

2 — Small Loop Impedance

The general form of the loop impedance with just radiation loss is,

$$Z_{loop} = \eta_0 \frac{\pi}{6}(kb)^4\left[1+8(kb)^2\right]\left[1-\frac{a^2}{b^2}\right]+\cdots$$
$$+j\omega\left[\mu_0 b\left[\ln\left(\frac{8b}{a}\right)-2+\frac{2}{3}(kb)^2\right]+M_{12}\right]\left[1+2(kb)^2\right] \quad (10)$$

including terms due to conductor thickness, and to the first-order current variation. The radian frequency is ω, and μ_0 is the free space permeability. M_{12} is the mutual coupling inductance between the primary and secondary loops obtained using the Neumann formula.

The *loaded* radiation Q of the antenna is,

$$Q_{rad} = \frac{1}{2}\frac{\mathrm{Im}\{Z_{loop}\}}{\mathrm{Re}\{Z_{loop}\}} \quad (11)$$

The primary loop loss resistance is,

$$R_{loss} = \frac{b}{a\delta\sigma} \quad (12)$$

where the σ is the loop conductivity in S/m, and the skin depth for good conductors is,

$$\delta = \sqrt{\frac{2}{\omega\mu_0\sigma}} \quad (13)$$

The Q_c of the resonating capacitor also contributes to losses in the form of parallel resistance across the capacitor, so that the net loaded Q_L of the antenna is,

$$Q_L = \frac{0.5}{\frac{1}{Q_C} + \frac{\mathrm{Re}\left\{Z_{loop}\right\} + R_{loss}}{\mathrm{Im}\left\{Z_{loop}\right\}}} \tag{14}$$

from which we can determine the loop current amplitude term I_0 for a given transmitter-supplied RF power P,

$$I_0 = \sqrt{\left(\frac{P}{R_{rad}}\right)\left(\frac{Q_L}{Q_{rad}}\right)} \tag{15}$$

The efficiency *eff* of the loop antenna follows as,

$$eff = \frac{I_0^{\,2} R_{rad}}{P} = \frac{Q_L}{Q_{rad}} \tag{16}$$

The value of Q_L can be obtained from Eqn. (14) or from direct measurements.

3 — The Secondary Feeding Loop

The secondary feeding loop has two main effects on the system. First, the total loop inductance increases by the mutual coupling inductance, M_{12}, between the primary loop and the secondary feeding loop. The result is that less capacitance is needed to resonate the antenna than if just the primary loop inductance were considered. Second, the relative diameters of the secondary feeding loop and the primary loop step up the primary loop resonant radiation plus loss resistance to the feed point value needed to match the feeding coax cable.

We used the Jordan and Balmain[10] high frequency extension to the Neumann formula, specialized to circular loops with constant current, to find the mutual coupling M_{12} between the primary loop and the secondary feeding loop.

$$M_{12} = \int_0^{2\pi}\int_0^{2\pi} \frac{b_2 b D_{12} \exp(-jkR_g)}{R_g} d\theta_1 d\theta_2 \tag{17}$$

and D_{12} and R_g are function of θ_1 and θ_2, the angles around the circumferences of the two loops,

$$D_{12} = \cos(\theta_1)\cos(\theta_2) + \sin(\theta_1)\sin(\theta_2) \tag{18}$$

and R_g further depends on the relative displacements of the two loops,

$$R_g = \sqrt{\left[b_2 \sin\theta_2 - b\sin\theta_1 + X\right]^2 + \cdots \\ + \left[b_2 \cos\theta_2 - b\cos\theta_1 + Z\right]^2 + Y^2} \tag{19}$$

where X, Y, and Z are the center-to-center displacement distances of the two loops that are in the zx plane. We solved Eqn. (17) using direct numerical integration in *Mathcad* software and include that solution on the **/qex-files** web page. For our loop dimensions, $(L_{self}+M_{12})/L_{self}$ is 1.02. M_{11} is the self-inductance of the primary loop. M_{12} is 57.3 nH for our example, and the loop centers are displace in the loop plane by 0.343 m.

Eqn. (17) can also be used to compute the complex self inductance L_{self} of the primary loop. Then, $j\omega L_{self}$ provides another way to compute the primary loop radiation impedance and reactance for a constant loop current.

4 — Fields at the Loop Center and in the Far Field Null

The electric field perpendicular to the surface of the wire is proportional to the rate of change (differentiation) of the current in the circumferential ϕ direction around the loop. Since we've included a loop term that varies with $\cos(\phi)$, thus survives differentiation in ϕ, we can derive a expression for the electric field in the center of the loop plane. Likewise, we can analyze the far field of the loop in the far-field null direction. In both cases the solution originates with the $2(C_\lambda)^2\cos(\phi)$ term of the loop current.

4.1— Fields at the Loop Center

The electric field at the center of the loop in the zx plane is found from the derivative with respect to ϕ of the loop current. Stated at the loop center $(x, y, z) = (0, 0, 0)$,

$$E_\phi(0,0,0) = -j\frac{\eta_0 k I_0}{2} \tag{20}$$

and the magnetic field can be approximated from the single-turn solenoid equation,

$$H_z(0,0,0) = \frac{I_0}{2b}\ . \tag{21}$$

The electric field depends on wavelength (via k) but does not depend on any loop dimension. The magnetic field, however, depends on the loop radius b. The wave impedance Z_W at the loop center is a measure of how well the loop discriminates between the electric and magnetic fields. That wave impedance is,

$$Z_W = \frac{E_\phi}{H_z} = -j\eta_0 kb = -j\eta_0 C_\lambda \tag{22}$$

clearly revealing the dependence of Z_W on the loop circumference. Also, because the electric field at (0, 0, 0) depends on the *variation* in the loop current, we would not be able to formulate an expression for the wave impedance from just a constant current term.

4.2— The Far-field Null

We evaluated the fields very far from the antenna using the exact analytical expressions in *Mathcad* to determine the loop peak-to-null ratio, and validated the results by NEC simulations. The far-field peak-to-null ratio depends on the current variation term in a simple manner for $C_\lambda < 0.3$. Stated in decibels the peak-to-null ratio of the small loop is,

$$N_{dB} = -20\log(2C_\lambda) \tag{23}$$

Table 2 shows the null depth across the 7 to 30 MHz operating range of our example loop. We compared the null depth using the simple formula of Eqn. (23), a detailed loop near-field calculation in *Mathcad*, and the null calculated from the 4*nec*2 model. The null becomes monotonically and smoothly shallower as the frequency increases for a fixed-size loop. This is normal and expected; recall that at $C_\lambda = 1$ we have the popular full-wavelength loop that exhibits gain of about +4 dBi in the broadside direction. Omitting the current variation term results in an erroneous prediction of an infinitely deep null.

The formula and analysis rely on the first term of the current variation, while the NEC result calculates the exact loop current. The single additional Fourier term loop current approximation becomes less reliable as frequency increases, but is still viable up to 30 MHz. As a result, we estimate that our loop current including a single variation term is reasonably accurate up to at least $C_\lambda = 0.3$.

5 — Loop Coupling to the Coax Feed Line

The secondary loop is fed directly with unbalanced coaxial cable, so there is opportunity to generate common mode currents on the coax feed line. We modeled the primary loop, secondary loop and coax outer shield in 4*nec*2, as rendered in Figure 1. We then varied the length of the

Table 2.
The null depth becomes progressively shallower as the frequency increases.

f, MHz	*Null [Eq. (23)], dB*	*Null [analysis], dB*	*Null [4nec2], dB*
7	17.52	17.52	17.50
10	14.42	14.57	14.50
14	11.50	11.41	11.47
18	9.32	9.29	9.12
21	7.98	7.94	7.83
24	6.82	6.77	6.76
30	4.88	4.79	4.13

coax and searched for the maximum current on the coax cable shield, just like on a previous study involving common mode currents (CMC) on the feed line to a dipole[11] that lacked a current choke.

5.1 — Common Mode Currents on the Feed Line

In this loop antenna, the CMCs are generated at the connection of the coax feed directly to the secondary loop. The CMCs appear to end-feed the shield of the coax feed line. We would expect a maximum coupling to a half-wavelength long feed line. Indeed, Figure 3 shows that the maximum CMC occurs for a coaxial feed line length of 0.45 λ.

We considered a loop that had a fixed coaxial cable length of about 3.3 m — or 0.08 λ at 7 MHz and 0.33 λ at 30 MHz — so if a common mode choke were to be used, it should be located on the coax cable at least a loop diameter away from the loop antenna, perhaps somewhere between 0 and 1.5 m from the transmitter end of the 3.3 m long coax cable.

5.2 — Measuring Loop Currents

We attempted to measure the loop currents and the feed line CMC at 14 and 28 MHz for the loop with its 3.28 m coaxial feed cable, and for an extended cable 9.61 m in length, as close as we could get to 0.452 wavelengths at 14 MHz, the length corresponding to a peak current in Figure 3. One of us, (W4RQ) constructed a 2.5 cm diameter current probe for the task.

We were able to measure in the 20 m band that the primary loop current was stronger than the feed loop current, and that the primary loop current varies along the circumference with the upper half of the loop (near the secondary feeding loop, 180º in Figure 2) having a slightly greater value than the lower half.

Due to the relative insensitivity of our homebrew *H*-field probe, we found no discernible CMCs on the feed-line, either for a long (9.61 m) or short (3.28 m) coaxial cable. With the long (nearly $\lambda/2$) feed line length, the loop tuning was exceptionally "touchy" and unstable.

6 — Vertical Loop Coupling to the Ground

We used the Neumann formula, Eqn. (17) with b_2 set to b, and a displacement between the loops to resemble a loop center-to-center distance to its image in the ground. We estimated the loop coupling to the ground by calculating the mutual inductance between the primary loop and its image in the ground, normalized to the loop self inductance and expressed in percent. That coupling affects the impedance of the loop antenna system. There is also a ground reflection, quite apart from the mutual coupling to ground, that affects the radiation pattern in the elevation plane. Here we are concerned only with the mutual coupling term that affects impedance.

Placing the loop above a perfect electric conducting (PEC) ground results in the strongest coupling. We also estimated the coupling for the "average" ground (σ = 0.005 S/m, ε_r = 13), and to a "poor" ground (σ = 0.001 S/m, ε_r = 5), by reducing the PEC coupling by the magnitude of the refection coefficient for normal incidence on the ground. The reflection coefficient magnitude is 1.0 for the PEC ground, 0.593 for the "average" ground and 0.393 for "poor" ground dielectric parameters at 14.1 MHz. Figure 4 shows the ratio of the mutual coupling to the self inductance in percent, a measure of ground coupling analogous to the ratio of mutual impedance to self impedance for a vertical dipole above ground.

Even for a PEC ground the coupling is less than 0.5% for a loop with its center more than one loop diameter above ground — where the bottom of the loop is a loop radius above ground. Using parameters for "real" ground further reduces that apparent mutual coupling. A loop with its center more than one loop diameter above ground is essentially independent of ground coupling as far as the effect on impedance and loop tuning is concerned. Note that ground reflections, quite apart from ground coupling, do have a significant effect on the loop antenna patterns.

7 — Efficiency of the Small Loop

We compared three methods to estimate the radiation efficiency of the small loop. In one *calculated* method we analytically determined the total loaded Q_L using Eqn. (14) and compared that to the loaded Q_{rad} of Eqn. (11), and then applied Eqn. (16) for the efficiency.

In a second method we measure *loaded* Q_L using a matched transmitter, and the classic bandwidth formula,

$$Q_L = \frac{\sqrt{F_H F_L}}{F_H - F_L} = \frac{\text{Frequency}}{\text{Bandwidth}} \tag{24}$$

where, given the antenna impedance, $Z = R + jX$ then F_H is the

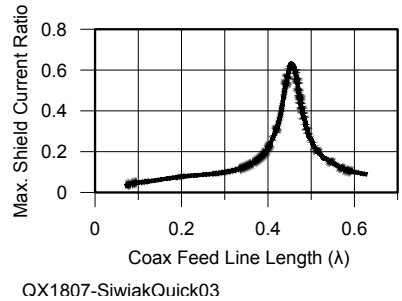

Figure 3 — Simulations using an NEC model of the loop antenna system of Figure 1 show that the maximum common mode current on the feeding cable has a strong but narrow peak for cable lengths that are near the half-wave resonant length.

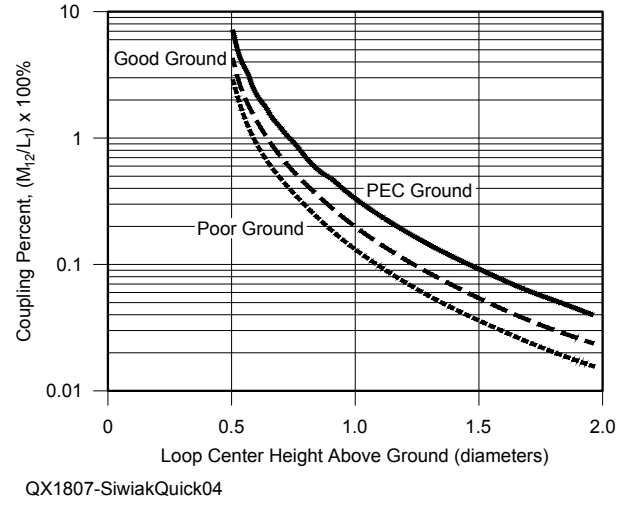

Figure 4 — The percent coupling to ground for this small HF loop is insignificant when the loop center is at least one loop diameter above the ground. Coupling is strongest for a PEC ground, and decreases significantly for realistic ground parameters.

frequency where $R = X$, and F_L is where $R = -X$, so that $F_H - F_L$ is the 3 dB bandwidth. F_H and F_L correspond to the 2.236:1 VSWR and the 7 dB return loss points. When the reactance does not cross zero, we can apply the incremental impedance formula,

$$Q = \frac{f}{2}\frac{|\Delta Z/\Delta f|}{R} \tag{25}$$

where for a small antenna, $|\Delta Z/\Delta f|$ is the magnitude of the incremental change in impedance Z divided by the incremental change in frequency f; and R is the resistance, or $\mathrm{Re}\{Z\}$ at frequency f. We then applied Eqn. (16) for the efficiency. These two approaches are the Q-method[12] for measuring efficiency.

Finally, we used the NEC model to simulate the efficiency. Figure 5 shows that all three methods of determining efficiency are within 0.5 dB of each other across 7 to 29 MHz, inspiring confidence in the analysis and in the NEC model.

The loop loss and radiation resistances increase with frequency. When resonated by the tuning capacitor, and transformed by mutual coupling to the feeding loop, the result is nearly constant input impedance across the operating frequencies. This is one of the key characteristics taught by Dunlavy in his 1971 patent. The secondary loop diameter and location bear an optimum relationship to the diameter of the primary loop so that variation in feed impedance is minimized over the band of operation.

8 — Conclusions

We introduced new improved formulas for the small HF loop current, and for the loop impedance by including one additional term of the Fourier series expansion for the loop current. That term is needed to adequately describe the current for loops up to 0.3 wavelengths in circumference. Including the additional Fourier term results in simple and accurate expressions for (1) the ratio of the electric-to-magnetic fields (field impedance Z_W) at the exact center of the loop, and (2) the far-field null depth.

CMCs on the feed line are small (negligible) as long as the feeding coax cable is not longer than the 3.3 m (less than 0.33 λ at the upper frequency extreme) length supplied with our example loop. CMC chokes, if used, could be attached between the transmitter end of the coax and up to 1.5 m from the transmitter end of the 3.3 m long cable.

Coupling of the vertical loop to a PEC ground is small, and decreases for realistic ground parameters, especially if the loop center is at least a loop diameter above ground. The loop coupling to ground, distinct from ground reflections that affect the elevation patterns, affects only the impedance match, which then requires a very small retuning of the loop.

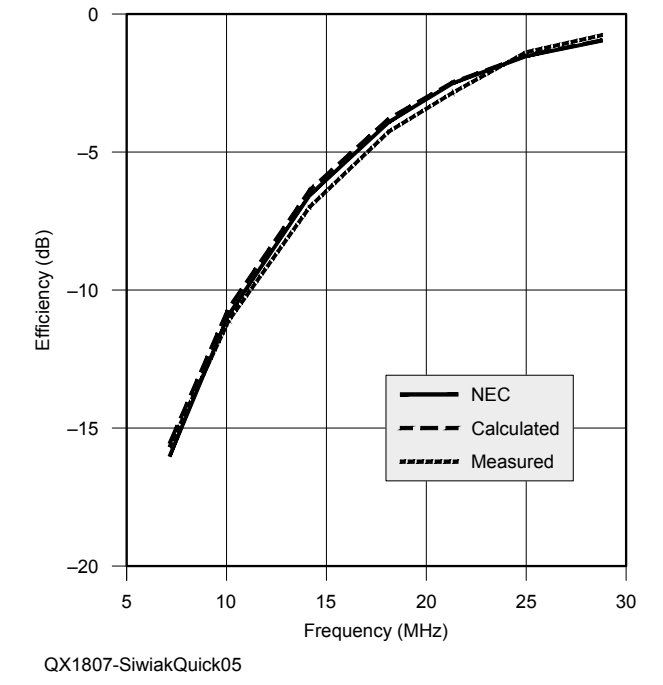

Figure 5 — Small loop efficiency simulated in NEC (solid), calculated from loop equations (long dashes), and measured using the Q method (short dashes). The close agreement among three methods validates the analysis, the Q measurements, and the completely independent NEC model.

Kazimierz (Kai) Siwiak, KE4PT, earned his PhD from Florida Atlantic University, Boca Raton, FL, specializing in antennas and propagation. He is a registered Professional Engineer and Life Senior Member of IEEE. Dr. Siwiak holds 41 US patents, has authored many peer-reviewed papers, several textbooks, and has contributed chapters to other books. Kai holds an Amateur Extra class license, is a life member of AMSAT, and member of ARRL where he serves on the RF Safety Committee and as Technical Advisor. He is a QST Contributing Editor, and Editor of QEX. Kai is a dedicated DXer and enjoys portable operating. His interests include flying (instrument and multiengine commercial pilot), hiking, and camping.

Richard Quick, W4RQ, is a retired Electronics and Metrology Engineering Technician. He was first licensed in 1977, and now holds the Amateur Extra class license. Richard is a member of the ARRL. He has built and tested several small loop transmitting antennas, studying the effects of using various materials and components, and has modeled them using Numerical Electromagnetic Code. Richard has co-authored the articles, "Does Your Antenna Need a Choke or Balun?" (QST, March 2017) and "Live Trees Affect Antenna Performance" (QST, February 2018). Richard enjoys operating at low power levels and from portable locations. He is an avid CW operator.

Notes

[1]John H. Dunlavy, Jr., "Wide Range Tunable Transmitting Loop Antenna", *US Patent 3,388,905*, issued June 28, 1971.
[2]H. C. Pocklington, "Electrical oscillations in wires," *Proc. Cambridge Phil. Soc.*, vol. 9, pp. 324-333, 1897.
[3]E. Hallén, "Theoretical investigation into transmitting and receiving qualities of antennae," *Nova Acta Regiae Soc. Ser. Upps.*, vol. II, pp. 1-4 , Nov. 4, 1938.
[4]J. E. Storer, "Impedance of thin-wire loop antennas," *Trans. AIEE*, vol. 75, pp. 606-619, Nov. 1956.
[5]Q. Balzano and K. Siwiak, "The Near Field of Annular Antennas," *IEEE Trans. Veh. Tech.*, Vol. VT-36, Nov. 1987, pp. 173-184.
[6]K. Siwiak, "Loop Antennas," in John G. Proakis (Ed.), **Wiley Encyclopedia of Telecommunications**, New York, NY: John Wiley & Sons, 2002, pp. 1290-1299.
[7]F. E. Neumann, "Allgemeine Gesetze der inducirten elektrischen Ströme [General laws of electrically induced currents]", *Treatises of the Royal Academy of Sciences in Berlin*, *Annalen der Physik*, 1846, vol. 143, issue 1, pp. 31-44.
[8]The *4nec2* NEC based antenna modeler and optimizer, by Arie Voors, **www.qsl.net/4nec2**.
[9] P. Salas, AD5X, Short Takes: The AlexLoop Walkham Portable Antenna, *QST*, Nov., 2013, p. 67.
[10]E.C. Jordan and K. G. Balmain, Section 14.16, p. 598, **Electromagnetic Waves and Radiating Systems, Second Edition**, Prentice–Hall, Inc., Englewood Cliffs, NJ.
[11]R. Quick, W4RQ, and K. Siwiak, KE4PT, "Does Your Antenna Need a Choke or a Balun?", *QST*, Mar, 2017, pp. 30-33.
[12]A. Findling, K9CHP and K. Siwiak, KE4PT, "How Efficient is Your QRP Small Loop Antenna?", *QRP Quarterly*, Summer 2012.
[13]K. Siwiak, KE4PT, "Q and the Energy Stored Around Antennas", *QST*, Feb., 2013, pp 37-38.